

## Supporting Information

### **Mitochondria-targeted Ir@AuNRs as bifunctional therapeutic agents for hypoxia imaging and photothermal therapy**

Libing Ke,<sup>‡a</sup> Cheng Zhang,<sup>‡a</sup> Xinxing Liao,<sup>a</sup> Kangqiang Qiu,<sup>a</sup> Thomas W. Rees,<sup>a</sup>

Yu Chen,<sup>\*,a</sup> Zizhuo Zhao,<sup>\*,b</sup> Liangnian Ji<sup>a</sup> and Hui Chao<sup>\*,a,c</sup>

<sup>a</sup> MOE Key Laboratory of Bioinorganic and Synthetic Chemistry, School of Chemistry, Sun Yat-Sen University, Guangzhou, 510275, P. R. China. E-mail:

[ceschh@mail.sysu.edu.cn](mailto:ceschh@mail.sysu.edu.cn), [chenyu63@mail.sysu.edu.cn](mailto:chenyu63@mail.sysu.edu.cn)

<sup>b</sup> Department of Ultrasound, Sun Yat-Sen Memorial Hospital, Sun Yat-Sen University, Guangzhou 510275, P. R. China. E-mail: [zhaozizh@mail.sysu.edu.cn](mailto:zhaozizh@mail.sysu.edu.cn)

<sup>c</sup> MOE Key Laboratory of Theoretical Organic Chemistry and Functional Molecule, School of Chemistry and Chemical Engineering, Hunan University of Science and Technology, Xiangtan, 400201, P. R. China.

<sup>‡</sup> These authors contributed equally to this work.

**11 March 2020**

**Note added after first publication:** This Supplementary Information file replaces that originally published on 05 August 2019, in which an incorrect image was included in Fig. S22. The light microscopy image for the brain sample treated with saline was duplicated in error for the brain sample treated with saline + NIR. The correct image has been included in this updated version, and the scale bars have also been added.

# Table of content

Experimental Section .....	4
<b>Materials</b> .....	4
<b>General instruments</b> .....	4
<b>Synthesis and Characterization</b> .....	5
<b>Synthesis of (E)-4-((2,2'-bipyridin)-4-yl diazenyl)phenol (bpy-OH)</b> .....	5
<b>Synthesis of (E)-4-((4-((10-bromodecanyl)oxy)phenyl) diazenyl)-2,2'-bipyridine (bpy-Br)</b> ..	5
<b>Synthesis of 10-(4-((4-(2,2'-bipyridin) diazenyl)phenoxy)decanyl)thioacetate (bpy-SAc)</b> ..	6
<b>Synthesis of 10-(4-((4-(2,2'-bipyridin) diazenyl)phenoxy)decanyl)thiol (bpy-SH)</b> .....	6
<b>Synthesis of [Ir(ppy)<sub>2</sub>(bpy-SH)]Cl (Ir-azo)</b> .....	7
<b>Synthesis of AuNRs and Ir@AuNRs</b> .....	7
<b>Determination of the number of Ir molecules per gold nanorod</b> .....	8
<b>Preparation of rat liver microsomes and procedure for Ir-azo to azo-reductase detection.</b> .....	9
<b>Photothermal performance of Ir@AuNRs after reduction.</b> .....	9
<b>Cell culture under normoxia and hypoxia</b> .....	9
<b>Cellular imaging of hypoxia and subcellular organelle co-localization</b> .....	10
<b>Imaging of hypoxia in multicellular tumor spheroid.</b> .....	10
<b>Cell viability and cytotoxicity test by NIR photothermal treatment</b> .....	11
<b>Cellular uptake and distribution of AuNRs and Ir@AuNRs</b> .....	11
<b><i>In vivo</i> experiments</b> .....	12
<b><i>Ex vivo</i> histological examination</b> .....	13
<b>References</b> .....	13
<b>Scheme S1 Synthetic routes to Ir-azo and Ir@AuNRs.</b> .....	14
<b>Fig. S1 The ESI-MS spectrum and <sup>1</sup>H NMR spectrum of bpy-OH.</b> .....	15
<b>Fig. S2 The ESI-MS spectrum and <sup>1</sup>H NMR spectrum of bpy-Br.</b> .....	16
<b>Fig. S3 The ESI-MS spectrum and <sup>1</sup>H NMR spectrum of bpy-SAc.</b> .....	17
<b>Fig. S4 The ESI-MS spectrum and <sup>1</sup>H NMR spectrum of bpy-SH.</b> .....	18
<b>Fig. S5 The ESI-MS spectrum and <sup>1</sup>H NMR spectrum of Ir-azo.</b> .....	19
<b>Fig. S6 Emission and UV-Vis-NIR absorption spectra of Ir-azo and Ir@AuNRs before and     after reduction with microsome/NADPH</b> .....	20

<b>Fig. S7</b> Seletive hypoxia sensitive assay of <b>Ir-azo</b> .....	21
<b>Fig. S8</b> TEM, Hydrodynamic diameter and Zeta potentials of <b>AuNRs</b> and <b>Ir@AuNRs</b> ...	22
<b>Fig. S9</b> XPS spectra of <b>Ir@AuNRs</b> .....	23
<b>Fig. S10</b> ESI-MS spectrum of <b>Ir@AuNRs</b> after reduction with microsome/NADPH.....	24
<b>Fig. S11</b> Confocal luminenscent image of cells by <b>Ir-azo</b> and <b>Ir@AuNRs</b> in vitro under normoxia and hypoxia conditions. ....	25
<b>Fig. S12</b> Confocal images of 3D multicellular spheroids incubated with <b>Ir@AuNRs</b> .....	26
<b>Fig. S13</b> Photothermal performance of <b>Ir@AuNRs</b> before and after reduction.....	27
<b>Fig. S14</b> Confocal images of co-localization of <b>Ir@AuNRs</b> and LTG, and its Pearson's coefficient .....	28
<b>Fig. S15</b> The intracellular distribution of <b>AuNRs</b> and <b>Ir@AuNRs</b> .....	29
<b>Fig. S16</b> Confocal images of co-localization of <b>Ir@AuNRs</b> and MTG at different time points .....	30
<b>Fig. S17</b> Cell viability of HeLa cells treated with <b>AuNRs</b> and <b>Ir@AuNRs</b> .....	31
<b>Fig. S18</b> The photographs of real-time heating temperature of <b>AuNRs</b> and <b>Ir@AuNRs</b> in vitro . ....	32
<b>Fig. S19</b> Photothermal effect of <b>AuNRs</b> and <b>Ir@AuNRs</b> in vivo.....	33
<b>Fig. S20</b> Representative photographs of mice before and after various treatments for days. ....	34
<b>Fig. S21</b> <i>In vivo</i> antitumor effect.....	35
<b>Fig. S22</b> Histological stainiing and analysis of major organs .....	36

## Experimental Section

### Materials

All chemical reagents were used as follows. IrCl<sub>3</sub>, phenyl pyridine (ppy), 2,2'-bpy (bpy), phenol, 1,10-dibromodecane, potassium thioacetate, cetyltrimethyl ammonium bromide (CTAB), anhydrous chloroauric acid (HAuCl<sub>4</sub>), anhydrous silver nitrate (AgNO<sub>3</sub>), ascorbic acid (V<sub>c</sub>), sodium borohydride (NaBH<sub>4</sub>), 3-(4,5-dimethylthiazol-2-yl)-2,5-diphenyltetrazolium bromide (MTT), Diphenyleneiodonium chloride (DPI), Phosphate buffer saline (PBS) power were purchased from Sigma Aldrich and used directly. Commercially available mitochondrial and lysosome tracking-imaging agents, Mito-tracker Green (MTG) and Lyso-tracking Green (LTG), were purchased from ThermoFisher. 2,2'-bipyridin-4-amine (bpy-NH<sub>2</sub>) and cyclometalated Ir(III) chloro-bridged dimer [Ir(ppy)<sub>2</sub>Cl]<sub>2</sub> were obtained according to our previous work.<sup>[1,2]</sup> Ultrapure water from a Milli-Q system was used throughout all experiments. PBS solution was adjusted to pH = 7.4 before use.

### General instruments

<sup>1</sup>H NMR spectra were obtained by a superconducting fourier transform nuclear magnetic resonance spectrometry (Bruker Avance III, Varian, Switzerland) using tetramethylsilane (TMS) as reference for the chemical shifts in the spectra. Electro spray ionization mass spectrometry (ESI-MS) was performed on an LCQ system (Finnigan MAT, USA). High-resolution mass spectra were obtained by an Orbitrap-Fusion-Lumos high-performance liquid chromatography-mass spectrometry (Thermo Fisher, Fusion Lumos, USA). Microanalyses (C, H and N) were determined by Perkin-Elmer 240Q elemental analyzer. UV-Vis-NIR spectra and emission spectra were recorded on a spectrophotometer (Perkin-Elmer Lambda 850) and spectrofluorophotometer (PerkinElmer LS 55). The morphology images were characterized by transmission electronmicroscopy (JEOL, JEM-1400 Plus, Japan). HAADF-STEM and elemental mapping images were obtained by Spherical aberration

corrected transmission electron microscope (JEM-ARM200P, Japan). X-ray photoelectron spectroscopy (XPS) spectra were obtained on an X-ray photoelectron spectrometer (Thermo VG, ESCALab250, USA). Particle sizing and surface potential measurement were performed on dynamic light scattering and Zeta potential measurement (Brookhaven BI-200SM). Elemental quantitative analysis was determined by inductively coupled plasma mass spectrometry (ICP-MS). A diode laser (808nm) from Hi-Tech Optoelectronics Co., Ltd (Beijing, China) was used in this study. *In vivo* fluorescence images were recorded on an *in vivo* imaging system (IVIS, PerkinElmer, Lumina XRMS Series III, USA).

## Synthesis and Characterization

### Synthesis of (E)-4-((2,2'-bipyridin)-4-yl diazenyl)phenol (bpy-OH)

To a stirred solution of 4-amino-2,2'-bipyridine (680 mg, 4mmol, 1.0eq) in distilled water (20 mL) cooled in an ice bath, concentrated HCl (2 mL) was added. A solution of NaNO<sub>2</sub> (300mg, 4.4 mmol, 1.1 eq) in water (8 mL) was then added into the solution and stirred for approximately 1h. A pre-cooled mixture of phenol (410mg, 4.4 mmol, 1.1 eq) and NaOH (400 mg, 10 mmol, 2.5 eq) was added dropwise. The pH of the solution was adjusted to 10 with dilute NaOH (0.1 mol/L) and the solution was subsequently stirred for 1h. A red precipitate was formed after the pH was adjusted again with diluted HCl(0.1 mol/L) to 5. The crude product was collected by filtration, dried and purified by column chromatography on silica (100~200 mesh) with CH<sub>2</sub>Cl<sub>2</sub>-MeOH as eluent to give a yellow solid (610 mg, 2.2 mmol, 54%). Anal. Calcd. for C<sub>16</sub>H<sub>12</sub>N<sub>4</sub>O(%): C, 69.55; H, 4.38; N, 20.28. Found: C, 69.35; H, 4.43; N, 20.38. ESI-MS (MeOH) m/z: 276.1 [L+H]<sup>+</sup>. <sup>1</sup>H NMR (400 MHz, DMSO-*d*<sub>6</sub>, δ) 10.63 (s, 1H), 8.89 (d, *J* = 3.9 Hz, 1H), 8.75 (d, *J* = 4.1 Hz, 1H), 8.65 (s, 1H), 8.46 (d, *J* = 7.9 Hz, 1H), 8.04-7.90 (m, 3H), 7.82-7.76 (m, 1H), 7.55-7.47 (m, 1H), 7.00 (d, *J* = 8.1 Hz, 2H).

### Synthesis of (E)-4-((4-((10-bromodecanyl)oxy)phenyl) diazenyl)-2,2'-bipyridine (bpy-Br)

To a stirred solution of bpy-azo-OH (550 mg, 2 mmol, 1 eq) in acetonitrile, 1,10-dibromodecane (3.6 g, 12 mmol, 6 eq) and K<sub>2</sub>CO<sub>3</sub> were added. The mixtures were refluxed for 8 h and cooled to room temperature. The crude product was collected by filtration and purified by column chromatography on silica (100~200 mesh) with CH<sub>2</sub>Cl<sub>2</sub>-EtOAc as eluent to give an orange solid (745 mg, 1.5 mmol, 75%). Anal. Calcd. for C<sub>26</sub>H<sub>31</sub>BrN<sub>4</sub>O(%): C, 63.03; H, 6.31; N, 11.31. Found: C, 62.84; H, 6.38; N, 11.42. ESI-MS (MeOH) m/z: 497.45 [L+H]<sup>+</sup>. <sup>1</sup>H NMR (400 MHz, CDCl<sub>3</sub>, δ) 8.82 (d, *J* = 7.9 Hz, 1H), 8.78-8.77 (m, 1H), 8.74-8.72 (m, 1H), 8.46 (d, *J* = 8.1 Hz, 1H), 8.00-7.97 (m, 2H), 7.84 (m, 1H), 7.69 (m, 1H), 7.34 (m, 1H), 7.03-7.00 (m, 2H), 4.05 (t, *J* = 4.1 Hz, 2H), 3.40 (t, *J* = 7.9 Hz, 2H), 1.88-1.79 (m, 4H), 1.50-1.40 (m, 4H), 1.38-1.29 (m, 8H).

#### **Synthesis of 10-(4-((4-(2,2'-bipyridin)diazenyl)phenoxy)decanyl)thioacetate (bpy-SAc)**

To a stirred solution of bpy-azo-Br in acetonitrile (745 mg, 1.5 mmol, 1 eq), potassium thioacetate (855 mg, 7.5 mmol, 5 eq) was added. The reaction was stirred at 60<sup>o</sup>C under Ar atmosphere for 6 h. The crude product was collected by filtration and purified by column chromatography on silica (100~200 mesh) with CH<sub>2</sub>Cl<sub>2</sub>-EtOAc as eluent to give an orange solid (340 mg, 0.8 mmol, 54%). Anal. Calcd. for C<sub>28</sub>H<sub>34</sub>N<sub>4</sub>O<sub>2</sub>S(%): C, 68.54; H, 6.98; N, 11.42. Found: C, 68.76; H, 7.13; N, 11.54. ESI-MS (MeOH) m/z: 491.66 [L+H]<sup>+</sup>. <sup>1</sup>H NMR (400 MHz, CDCl<sub>3</sub>, δ) 8.84 (d, *J* = 4.1 Hz, 1H), 8.81 (d, *J* = 4.1 Hz, 1H), 8.75 (d, *J* = 4.1 Hz, 1H), 8.51 (d, *J* = 7.9 Hz, 1H), 8.01-7.98 (m, 2H), 7.88 (m, 1H), 7.72 (m, 1H), 7.37 (m, 1H), 7.04-7.01 (m, 2H), 4.06 (t, *J* = 4.1 Hz, 2H), 2.88-2.85 (m, 2H), 2.32 (s, 3H), 1.85-1.80 (m, 2H), 1.57 (m, 2H), 1.50-1.44 (m, 2H), 1.39-1.33 (m, 4H), 1.32-1.26 (m, 6H).

#### **Synthesis of 10-(4-((4-(2,2'-bipyridin)diazenyl)phenoxy)decanyl)thiol (bpy-SH)**

To a stirred solution of bpy-azo-SAc in CH<sub>2</sub>Cl<sub>2</sub> (245 mg, 0.5 mmol, 1 eq), a solution of KOH (200 mg) in methanol (10 mL) was added and stirred for 20 min. Then another solution of acetic acid (1 mL) in CH<sub>2</sub>Cl<sub>2</sub> (20 mL) was added in one

minute and subsequently stirred for 30 min. The reaction was terminated by adding 20 mL distilled water under vigorous stirring. The crude product in organic layer was washed with water three times, then collected and purified by column chromatography on silica (100~200 mesh) with CH<sub>2</sub>Cl<sub>2</sub>-EtOAc as eluent to give an orange solid (125 mg, 0.28 mmol, 56%). Anal. Calcd. for C<sub>26</sub>H<sub>32</sub>N<sub>4</sub>OS(%): C, 69.61; H, 7.19; N, 12.49. Found: C, 69.47; H, 7.27; N, 12.74. ESI-MS (MeOH) m/z:449.62 [L+H]<sup>+</sup>. <sup>1</sup>H NMR (400 MHz, CDCl<sub>3</sub>, δ)8.83 (d, *J* = 4.1 Hz, 1H), 8.79 (d, *J* = 3.9 Hz, 1H), 8.74 (d, *J* = 4.1 Hz, 1H), 8.48 (d, *J* = 3.9 Hz, 1H), 8.01-7.98 (m, 2H), 7.86 (m, 1H), 7.71 (m, 1H), 7.35 (m, 1H), 7.04-7.01 (m, 2H), 4.06 (t, *J* = 4.1 Hz, 2H), 2.52 (m, 2H), 1.86-1.80 (m, 2H), 1.61 (m, 2H), 1.51-1.45 (m, 2H), 1.39-1.34 (m, 4H), 1.32-1.26 (m, 7H).

### Synthesis of [Ir(ppy)<sub>2</sub>(bpy-SH)]Cl (Ir-azo)

The compound [Ir<sub>2</sub>(ppy)<sub>4</sub>Cl<sub>2</sub>] were synthesized according to literature methods.<sup>[1]</sup> [Ir<sub>2</sub>(ppy)<sub>4</sub>Cl<sub>2</sub>] (53 mg, 0.05 mmol, 1 eq) and bpy-azo(45 mg, 0.1 mmol, 2 eq) was dissolved in 20 mL CH<sub>2</sub>Cl<sub>2</sub>/MeOH (1:1, v/v), and the solution was refluxed overnight under Argon. The crude product was collected and purified by column chromatography on neutral aluminum oxide (200~300 mesh) with CH<sub>2</sub>Cl<sub>2</sub>-MeOH as eluent to give a red solid (81 mg, 0.082 mmol, 82%). Anal. Calcd. for C<sub>48</sub>H<sub>48</sub>ClIrN<sub>6</sub>OS(%): C, 60.74; H, 5.10; N, 8.85. Found: C, 60.53; H, 5.19; N, 8.64. ESI-MS (MeOH) m/z: 947.30 [M-Cl]<sup>+</sup>. <sup>1</sup>H NMR (400 MHz, CDCl<sub>3</sub>, δ)9.22 (d, *J* = 4.1 Hz, 1H), 9.15 (s, 1H), 8.54 (s, 1H), 8.04 (m, 3H), 7.94 (d, *J* = 4.1 Hz, 3H), 7.79 (m, 2H), 7.71 (m, 3H), 7.57-7.51 (m, 3H), 7.08-6.99 (m, 6H), 6.93 (m, 2H), 6.31 (m, 2H), 4.06 (m, 2H), 2.68 (t, *J* = 4.1 Hz, 2H), 1.81 (m, 2H), 1.67 (m, 2H), 1.49-1.44 (m, 2H), 1.40-1.34 (m, 4H), 1.32-1.24 (m, 7H).

### Synthesis of AuNRs and Ir@AuNRs

All glassware was washed with aqua regia and rinsed with distilled water before preparation. Gold nanorods were prepared using a seed-growth method according to the literature.<sup>[2]</sup> Cold NaBH<sub>4</sub>(0.6 mL, 10 mmol/L) was poured into a CTAB (1 mmol/L)

solution containing HAuCl<sub>4</sub> stock solution (0.1 mL, 25 mmol/L) and stirred vigorously to obtain the seed solution. Then, growth solution was prepared as followed. To a solution of CTAB (1 mmol/L), AgNO<sub>3</sub> (0.1 mL, 4 mmol/L), HAuCl<sub>4</sub> (0.3 mL, 25 mmol/L) and ascorbic acid (0.08 mL, 8 μmol/L) were added successively. The mixtures were gently stirred for seconds and then 10 μL of seed solution was added and left unshaken at room temperature. CTAB-capped AuNRs formed within 2 h and were dialyzed overnight to remove an excess of CTAB. **Ir-azo** (10 mg in 2 mL DMSO) was added into the **AuNRs** solution, and the solution stirred for 24 h to ensure the **AuNRs** surfaces were coated with Ir complex. Dialysis using a 3.5k MWCO membrane removed unreacted Ir complexes and give **Ir@AuNRs**.

The formation of **Ir@AuNRs** was characterized by UV-Vis-NIR, IR, TEM, and DLS.

### **Determination of the number of Ir molecules per gold nanorods.**

The Ir@AuNRs were completely digested by 1 mL of aqua regia at room temperature. Subsequently, the sample was diluted to 3% HNO<sub>3</sub> with MilliQ H<sub>2</sub>O, and then analyzed by ICP-MS. The number of Ir molecules per gold nanorods is calculated as follow:

$$N_{\text{AuNRs}} = \frac{m_{\text{AuNRs}}}{\rho_{\text{Au}} \cdot V_{\text{AuNRs}}}$$

$$V_{\text{AuNRs}} = \pi \left(\frac{W}{2}\right)^2 \cdot (L - W) + \frac{4}{3} \pi \left(\frac{W}{2}\right)^3$$

$$N_{\text{Ir}} = n_{\text{Ir}} \cdot N_{\text{A}} = \frac{m_{\text{Ir}}}{M_{\text{Ir}}} \cdot N_{\text{A}}$$

$$R = \frac{N_{\text{Ir}}}{N_{\text{AuNRs}}}$$

m: measured density of ions (atoms) from ICP-MS analysis (g/L)

ρ: density of Au

W: the width of AuNRs  
L: the length of AuNRs  
n: molar number  
M: molecular weight (g/mol)  
R: atomic percentage of Ir to AuNRs

## **Preparation of rat liver microsomes and procedure for Ir-azo to azo-reductase detection.**

Rat liver microsomes were extracted according to the method of Omura and Sato.<sup>[3]</sup> The liver was homogenized in three volumes of the same buffer. Microsomes (0.25mg protein/mL) and **Ir-azo** (2.5  $\mu$ M) or **Ir@AuNRs** (50  $\mu$ g/mL) were mixed and incubated in PBS at 37°C under hypoxic conditions by pre-excluding oxygen with Argon for 30 min. 50  $\mu$ M NADPH was added to the solution. The reaction mixture after *in vitro* reduction assay was extracted by chloroform and analysed by UV-Vis absorption spectra, emission spectra and ESI-mass spectra.

For selective reduction assay, a high concentration of bio-related molecules and ions (1mM of Cys, Hcy, GSH,  $\text{SO}_3^{2-}$ ,  $\text{HSO}_3^-$ ,  $\text{Cl}^-$ ,  $\text{Mg}^{2+}$ ,  $\text{Cu}^{2+}$ ,  $\text{Zn}^{2+}$ ,  $\text{Ca}^{2+}$ ,  $\text{K}^+$ ,  $\text{HCO}_3^-$ ,  $\text{NO}_2^-$ ,  $\text{NO}_3^-$ ,  $\text{PO}_4^{3-}$ ,  $\text{I}^-$ ,  $\text{ClO}_4^-$ ,  $\text{ClO}^-$ ,  $\text{S}^{2-}$ ,  $\text{CO}_3^{2-}$ ,  $\text{S}_2\text{O}_3^{2-}$ ,  $\text{S}_4\text{O}_6^{2-}$ ,  $\text{H}_2\text{O}_2$ ) were added to a PBS solution of 2.5  $\mu$ M Ir-azo and incubated for 30 min at 37 °C. The emission intensity was measured.

## **Photothermal performance of Ir@AuNRs after reduction.**

In order to measure the photothermal effect of **Ir@AuNRs** after reduction with microsomes/NADPH, an 808 nm NIR laser was used as laser source. 100  $\mu$ L of the reduced-**Ir@AuNRs** (50 $\mu$ g/mL) was prepared and irradiated for 5 min. The real-time temperature images were recorded by the infrared camera once every 30 s.

## **Cell culture under normoxia and hypoxia**

Human cervical cancer cells (HeLa cells) and Human lung adenocarcinoma cells (A549 cells) lines were purchased from the centre for experimental animals, Sun Yat-Sen University (Guangzhou, China). Cells were cultured at 37°C in 5% CO<sub>2</sub> in DMEM mixed with 10% premium fetal bovine serum (FBS) and 1% penicillin/streptomycin. For hypoxic condition incubation, adherent cells were transferred to a hypoxic incubator (5%, 3%, 1% O<sub>2</sub>) for 6 h, and used directly.

## **Cellular imaging of hypoxia and subcellular organelle co-localization**

A549 cells were pre-cultured in glass bottom dishes (35mm, Corning), then placed in hypoxia (5%, 3%, 1% O<sub>2</sub>). After further incubation with **Ir-azo** (2.5 μM) for 30 min or **Ir@AuNRs** (50 μg/mL) for 4 h, the culture medium was discarded and refreshed with PBS. Cell imaging was performed. For the organelle co-localization experiment, mitochondrial tracker green (MTG) and lysosome tracker green (LTG) were added to the cells for another 30 min after treatment with **Ir@AuNRs** (50 μg/mL). Confocal microscope (Zeiss LSM 880 NLO, 63x/NA 1.4 oil immersion objective) was employed to image the cells. The excitation wavelengths were 405 nm and 488 nm for the Ir complex and dyes (MTG and LTG), respectively. The collected emission signal was 570±20 nm for the Ir complex and 500±20 nm for the dyes.

## **Imaging of hypoxia in multicellular tumor spheroid.**

3D multicellular tumor spheroids (MCTSs) were formed in agarose-based 96-well plates according to previously method.<sup>[4]</sup> 50 μL of a 2.5 × 10<sup>4</sup> A549 cells/mL trypsin-digested cells were seeded onto agarose-based (1% (w/v) in PBS) 96-well plates. The cells were able to aggregate spontaneously, resulting in the formation of MCTSs with diameters varying from 400-500 μm for 96 h. To image the hypoxia region of 3D spheroids, MCTSs were treated with **Ir@AuNRs** for 4 h and then washed gently twice with PBS. The MCTSs were imaged using a confocal microscope (Zeiss LSM 880 NLO, 10 x objectives).

## **Cell viability and cytotoxicity test by NIR photothermal treatment**

Measurement of cell viability was carried out by MTT assay.  $1 \times 10^4$  cells per well were seeded on 96-well plates and incubated at 5% CO<sub>2</sub> at 37 °C for 24 h, allowing for sufficiently adherent growth. HeLa and A549 Cells were treated with different concentrations of **AuNRs** or **Ir@AuNRs** under hypoxia incubation, where PBS was used as control group. After incubation for 24 h, supernatant was removed and refreshed with fresh culture medium, and then MTT (20 $\mu$ L, 5mg/mL) was added. After incubation for 4 h, DMSO (200  $\mu$ L/well) was added to dissolve the purple formazan crystals. Absorbance at 595 nm was measured, and the assay was repeated 3 times.

For the measurement of PTT cytotoxicity, the as-incubated cells were treated with **AuNRs** and **Ir@AuNRs** under hypoxia for 4 h, followed by a supernatant wash-out procedure and irradiation with an 808 nm NIR laser at 0.8 W/cm<sup>2</sup>. The cells were then treated as above for the cell viability assay.

In order to visualize the photothermal effect, calcein-AM and Ethidium homodimer-1 were added to A549 cells for another 30 min after treatment with **AuNRs** and **Ir@AuNRs** (50  $\mu$ g/mL) to differentiate live/dead cells. The collected emission signal was 510 $\pm$ 20 nm for Calcein-AM and 610 $\pm$ 20 nm for EthD-1.

## **Cellular uptake and distribution of AuNRs and Ir@AuNRs**

Exponentially grown A549 cells in 10 mm petri dishes had their media removed and replaced with 10 mL DMEM before treatment with **AuNRs** and **Ir@AuNRs** (50 $\mu$ g/mL) for 4 h. The cells were then harvested by digestion with trypsin. After digestion with HNO<sub>3</sub> (60%) and H<sub>2</sub>O<sub>2</sub> (20%) for more than 24 h, all the samples were tested by ICP-MS to quantify the gold content.

For quantitative subcellular distribution, the **Ir@AuNRs**-treated cells were divided into two portions. A nucleus extraction kit and a cytoplasm extraction kit (Shanghai

Sangon Biological Engineering Technology & Services Co. Ltd.) were used on the portions. All samples were conducted the same manner as described above to quantify the content of gold and iridium.

For Bio-TEM imaging analysis, the **Ir@AuNRs**-treated cells were digested with trypsin and obtained by centrifuge. Then the solid cells were fixed in 0.1 M PBS containing 2.5% glutaraldehyde and 4% paraformaldehyde for 1 h, rinsed with distilled water, stained with 0.5% uranyl acetate for 1 h, dehydrated in a graded series of ethanol (30, 60, 70, 90 and 100%), and embedded in epoxy resin. The resin was polymerized at 60 °C for 48 h. Ultrathin sections (50-75 nm) obtained with a LKB ultramicrotome were stained with 2% aqueous uranyl acetate and 2% aqueous lead citrate. Bio-TEM images were obtained with transmission electron microscopy.

### ***In vivo* experiments**

Female Balb/c-(nu/nu) nude mice (8 weeks) were purchased from Beijing Vital River Laboratory Technology Co., Ltd. and use under the protocols approved by the Institutional Animal Care and Sun Yat-sen University Animal Care and Use Committee. Mice were stochastically divided into groups. A549 xenografts were formed by inoculating  $1 \times 10^6$  suspended cells *via* subcutaneous injection into the right hip of each nude mouse. When the tumour volume reached  $\sim 300 \text{ mm}^3$ , the nude mice were treated with different conditions.

To investigate the hypoxia-responsive capability of **Ir@AuNRs**, tumor-bearing mice were intratumorally injected with **Ir@AuNRs** (1 mg/kg), and then imaged at different time points by IVIS (Ex: 420 nm, Em: 570 nm).

To evaluate the effect of photothermal therapy, mice were divided into 6 groups with six mice per group. Different Groups were treated to quantify the growth rate of tumors: (1) Only saline; (2) saline +  $0.8 \text{ W/cm}^2$  808nm laser for 5min; (3) Only **AuNRs** (1 mg/kg); (4) **AuNRs** (1 mg/kg) +  $0.8 \text{ W/cm}^2$  808nm laser for 5 min; (5) Only **Ir@AuNRs** (1 mg/kg); (6) **Ir@AuNRs** (1 mg/kg) +  $0.8 \text{ W/cm}^2$  808nm laser for 5min. The weights of the mice and their tumor sizes were measured every 3 days after treatment. Tumor volume was calculated based on the following equation: Tumor

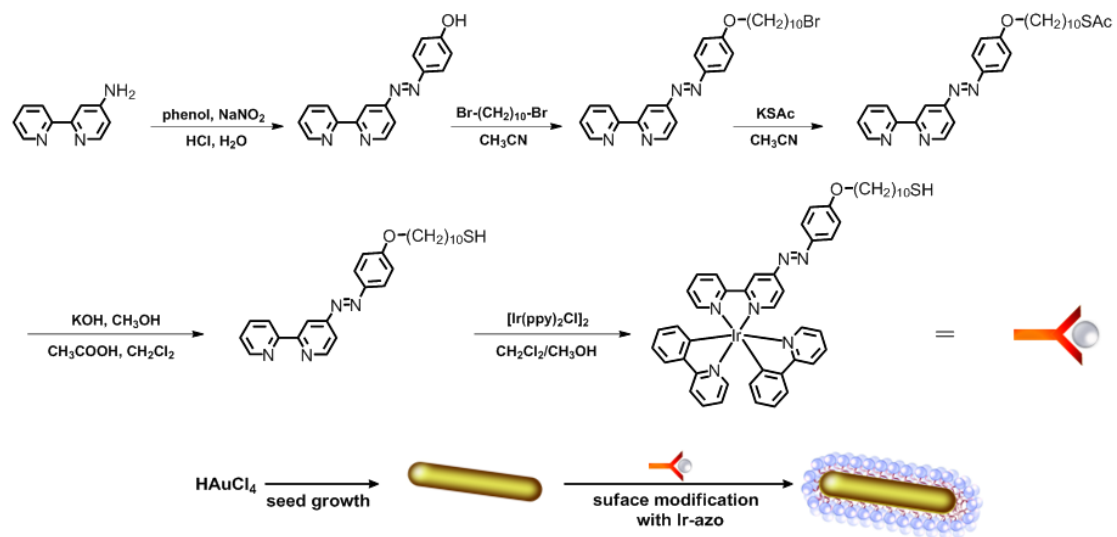
Volume (V) = width<sup>2</sup> × length × 0.5. Relative tumor volumes were calculated as V/V<sub>0</sub>. These data were plotted as a function of time.

### ***Ex vivo* histological examination**

All mice were sacrificed at the end of photothermal therapy. Tumours were collected and dissected from remaining tumor-bearing mice. The organs (brain, lung, heart, liver, kidney, spleen, and intestine) were resected and immersed in 4% paraformaldehyde at 4°C. For morphological studies, 6 µm sections were acquired from paraffin-embedded samples, processed according to the standard procedures for inclusion, and rehydrated (xylene, alcohol, water). The sections were stained with Hematoxylin-eosin (H&E) and observed with an Olympus microscope to analyze the tissue structure and cell state.

### **References**

- [1] Z. G. Zhou, G. H. Sarova, S. Zhang, Z. P. Ou, F. T. Tat, K. M. Kadish, L. Echegoyen, D. M. Guldi, D. I. Schuster and S. R. Wilson, *Chem. Eur. J.*, 2006, 12, 4241.
- [2] B. Nikoobakht and M. A. El-Sayed, *Chem. Mater.*, 2003, 15, 1957.
- [3] T. Omura and R. Sato, *J. Biol. Chem.* 1964, 239, 2370.
- [4] H. Y. Huang, P. Y. Zhang, H. M. Chen, L. N. Ji and H. Chao, *Chem. Eur. J.*, 2015, 21, 715.



**Scheme S1** Synthetic routes to **Ir-azo** and **Ir@AuNRs**.

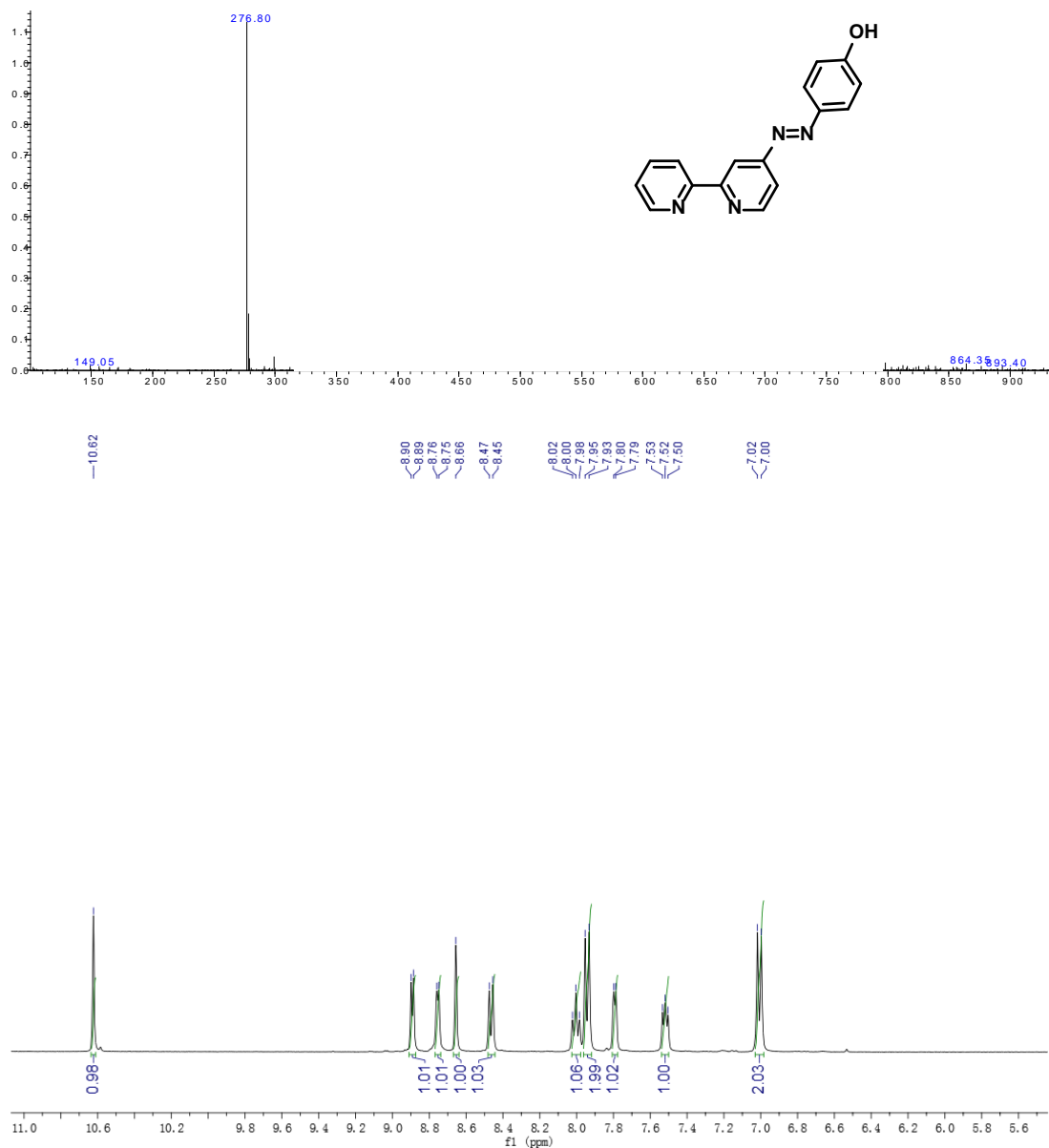


**Fig. S1** The ESI-MS spectrum and <sup>1</sup>H NMR spectrum of bpy-OH.

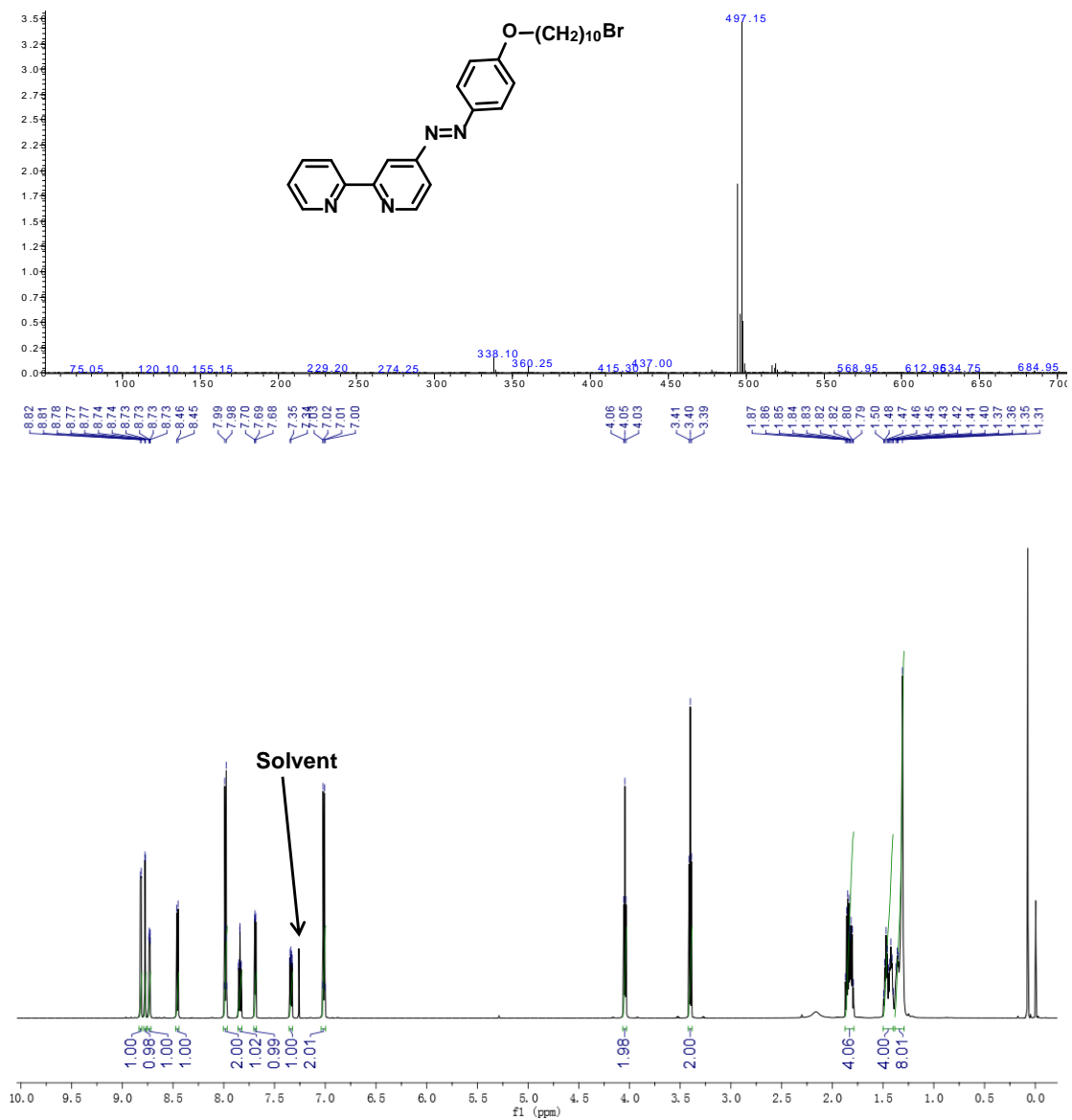


**Fig. S2** The ESI-MS spectrum and <sup>1</sup>H NMR spectrum of bpy-Br.

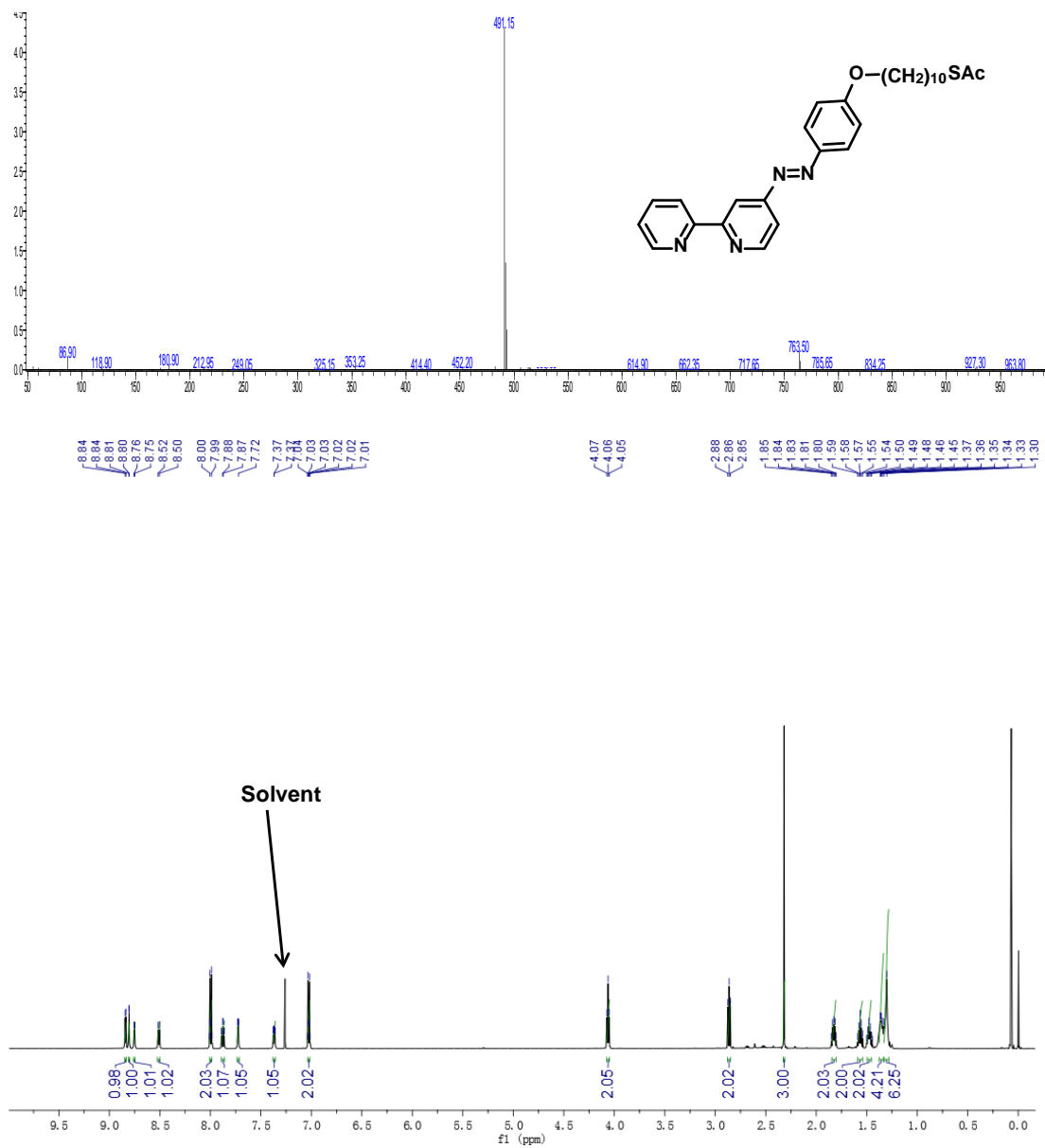


**Fig. S3** The ESI-MS spectrum and <sup>1</sup>H NMR spectrum of bpy-Sac.

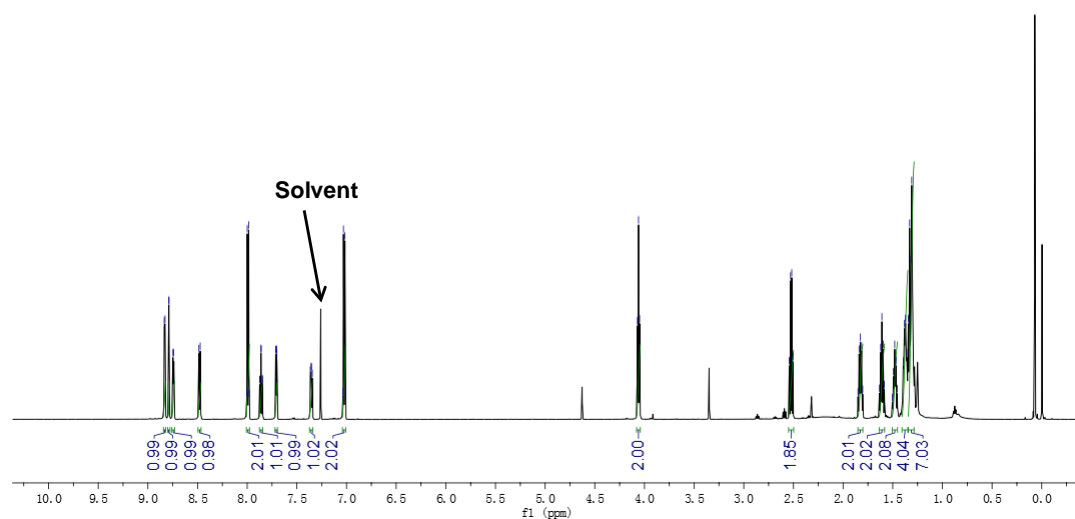
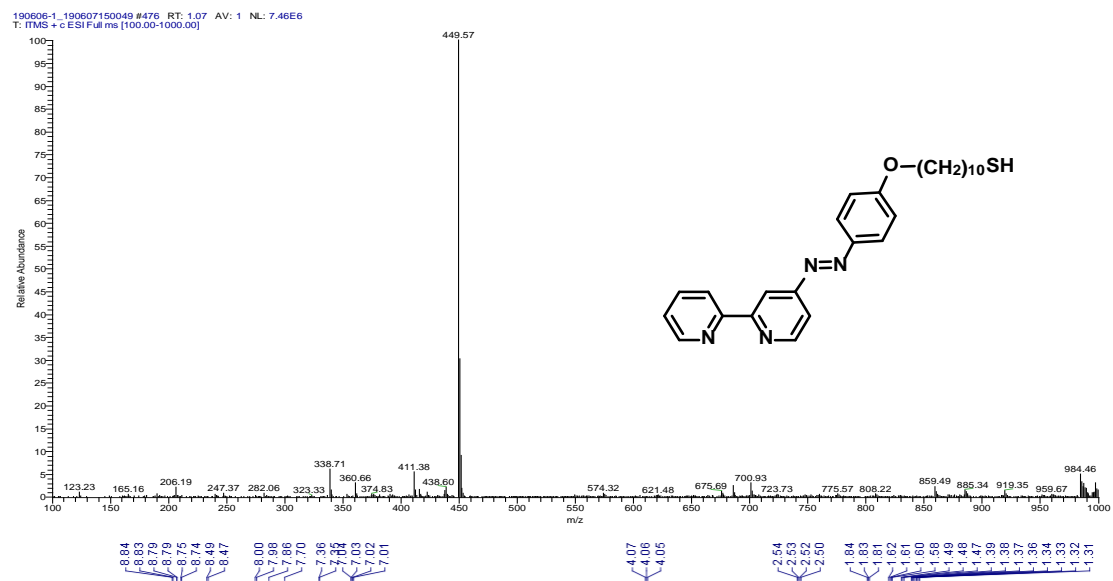


**Fig. S4** The ESI-MS spectrum and  $^1\text{H}$  NMR spectrum of bpy-SH.

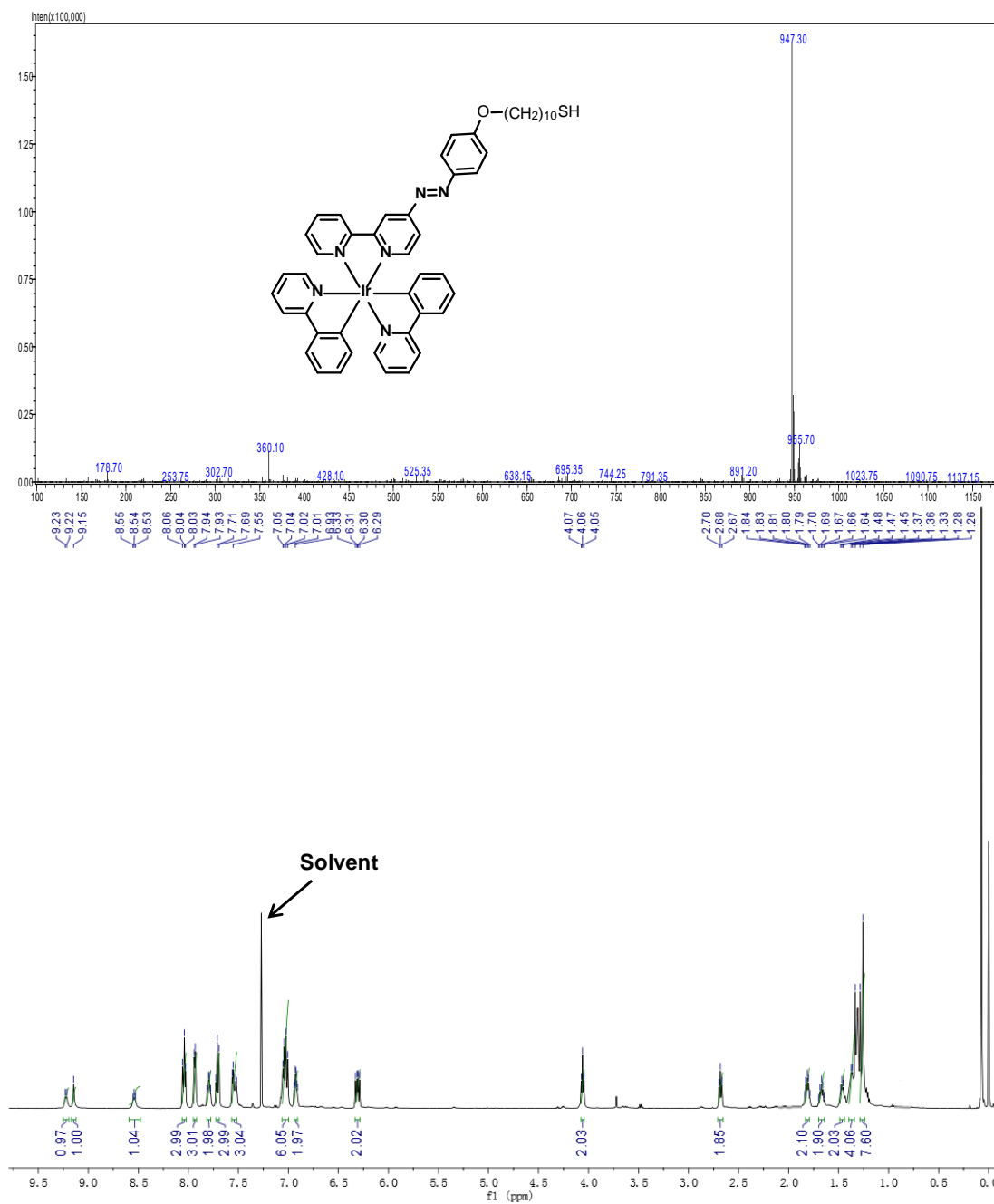


**Fig. S5** The ESI-MS spectrum and <sup>1</sup>H NMR spectrum of Ir-azo.

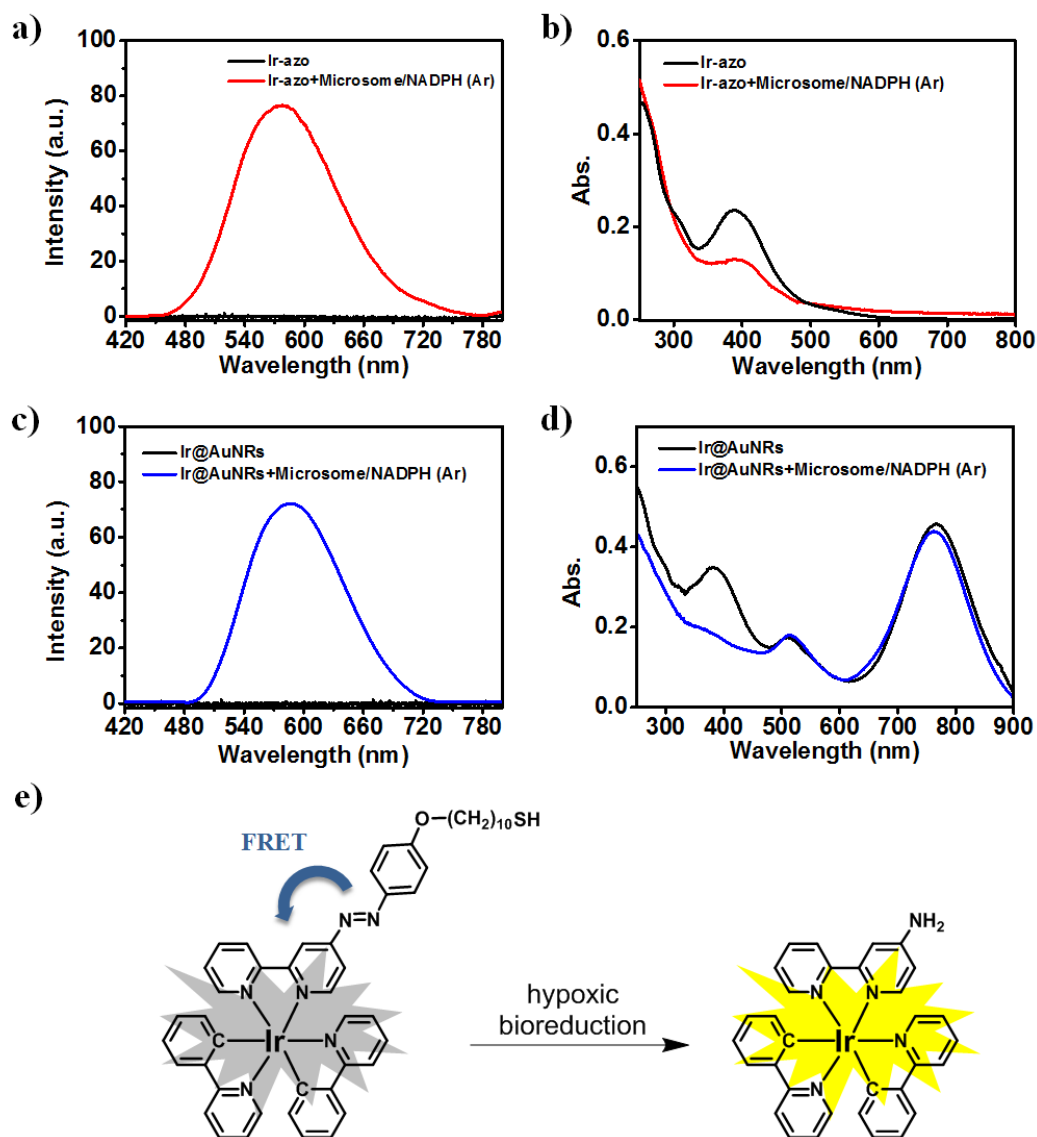


**Fig. S6** a) Emission and b) UV-Vis-NIR absorption spectra of **Ir-azo** in the presence of rat liver microsome/NADPH under normoxia (black) and hypoxia (red). c) Emission and d) UV-Vis-NIR absorption spectra of **Ir@AuNRs** in the presence of rat liver microsome/NADPH under normoxia (black) and hypoxia (blue). e) Reduction mechanism of **Ir-azo** to **Ir-NH<sub>2</sub>**.

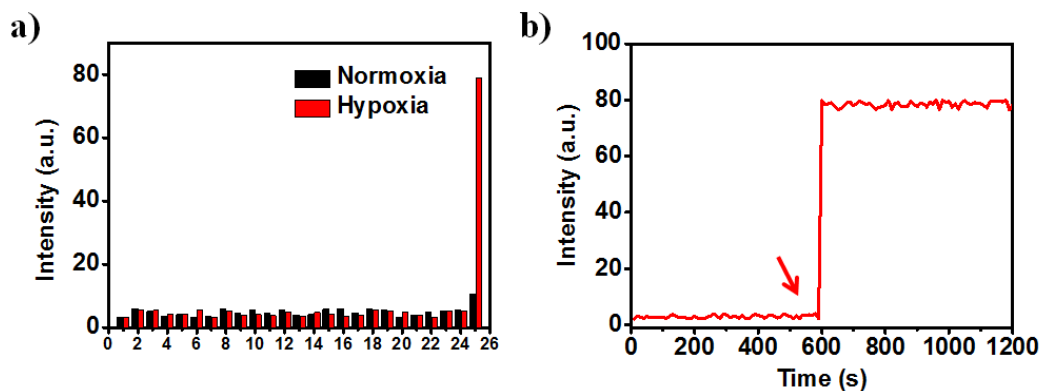


**Fig. S7** a) Phosphorescent intensity of 2.5  $\mu\text{M}$  **Ir-azo** in PBS buffer.  $\lambda_{\text{ex/em}} = 405$  nm/570 nm. Bars: 1, Control; 2, Cys; 3, Hcy; 4, GSH; 5,  $\text{Na}_2\text{SO}_3$ ; 6,  $\text{NaHSO}_3$ ; 7,  $\text{NaCl}$ ; 8,  $\text{MgCl}_2$ ; 9,  $\text{CuCl}_2$ ; 10,  $\text{ZnCl}_2$ ; 11,  $\text{CaCl}_2$ ; 12,  $\text{KCl}$ ; 13,  $\text{NaHCO}_3$ ; 14,  $\text{NaNO}_2$ ; 15,  $\text{NaNO}_3$ ; 16,  $\text{Na}_3\text{PO}_4$ ; 17,  $\text{NaI}$ ; 18,  $\text{NaClO}_4$ ; 19,  $\text{NaClO}$ ; 20,  $\text{Na}_2\text{S}$ ; 21,  $\text{Na}_2\text{CO}_3$ ; 22,  $\text{Na}_2\text{S}_2\text{O}_3$ ; 23,  $\text{Na}_2\text{S}_4\text{O}_6$ ; 24,  $\text{H}_2\text{O}_2$ ; 25, Microsomes/NADPH. b) Time-dependent changes of phosphorescence intensity of **Ir-azo** (2.5  $\mu\text{M}$ ) under normoxia and hypoxia. Data were measured at 37  $^\circ\text{C}$  in PBS containing rat liver microsomes and NADPH as a cofactor. NADPH was added at the point indicated by the arrow.  $\lambda_{\text{ex/em}} = 405$  nm/570.

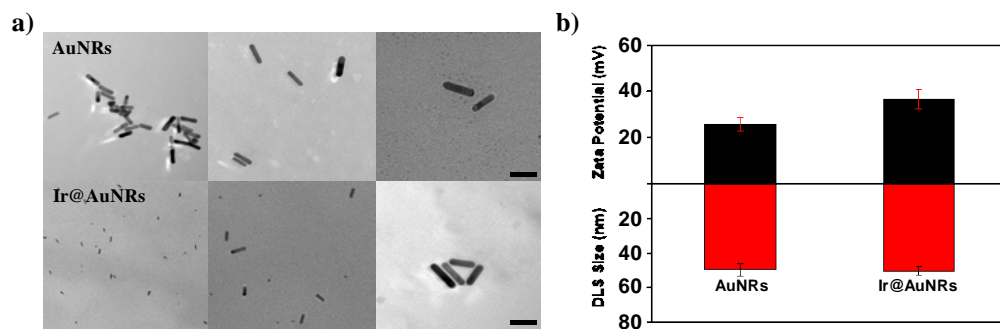


**Fig. S8** a) TEM image of **AuNRs** and **Ir@AuNRs**. Scale bar: 50 nm. b) Hydrodynamic diameter and Zeta potentials of **AuNRs** and **Ir@AuNRs**.

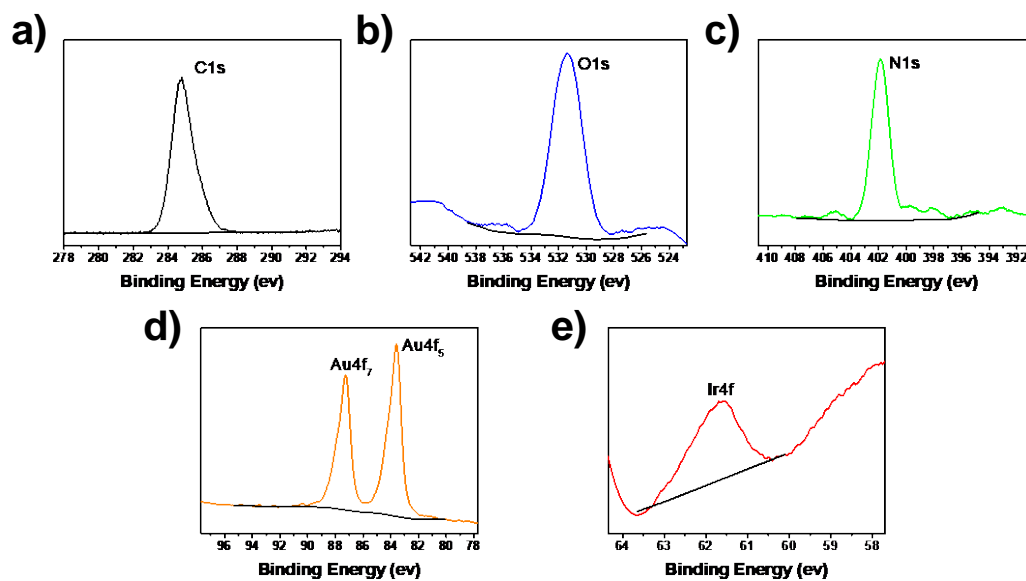


**Fig. S9** X-ray photoelectron spectra (C<sub>1s</sub>, O<sub>1s</sub>, N<sub>1s</sub>, Au<sub>4f</sub> and Ir<sub>4f</sub>) of Ir@AuNRs.

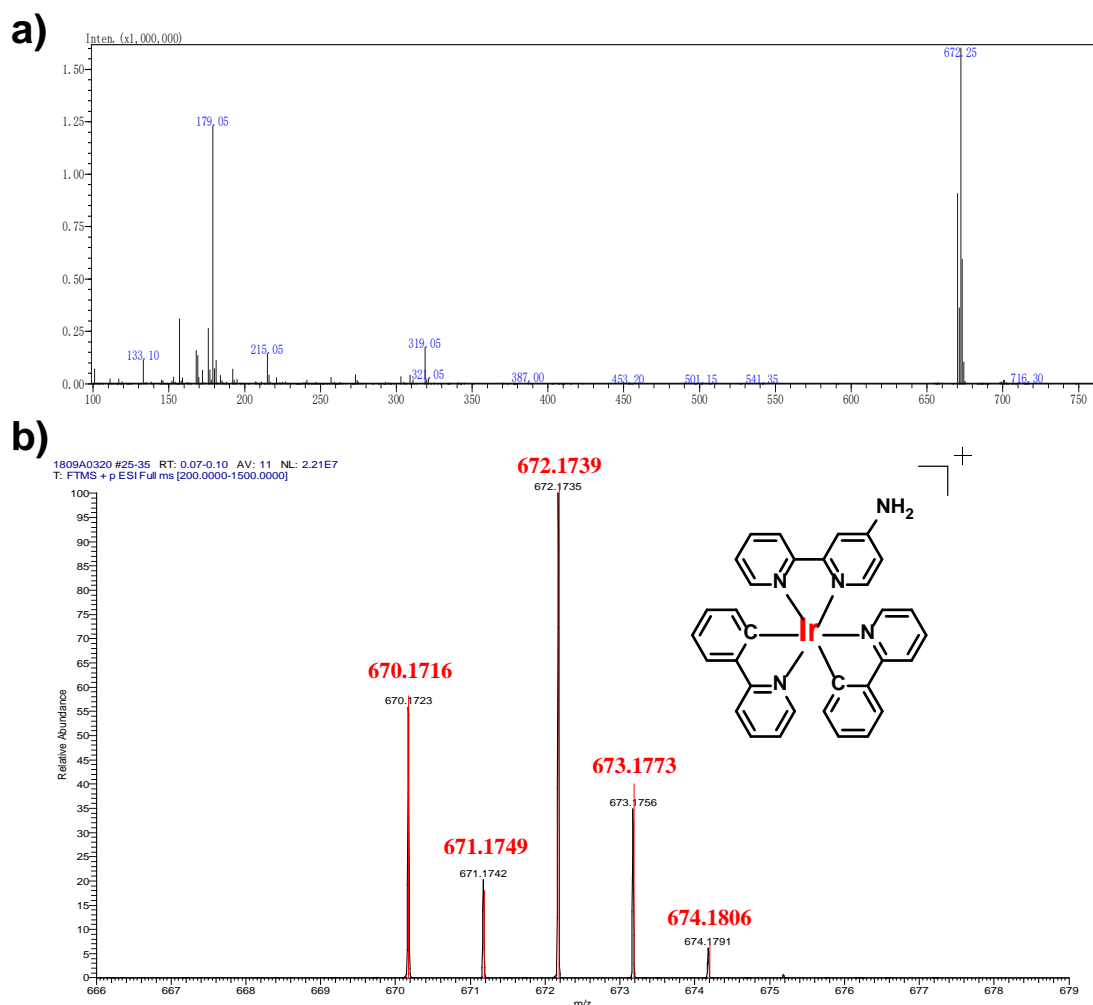


**Fig. S10** a) ESI-MS spectrum of the complex produced from **Ir@AuNRs** after incubation with rat liver microsomes/NADPH in PBS at 37 °C for 30 min. b) Zoom Scan MS spectra of iridium isotope peaks (black) of a) and the simulation (red) of **Ir-NH<sub>2</sub>**.

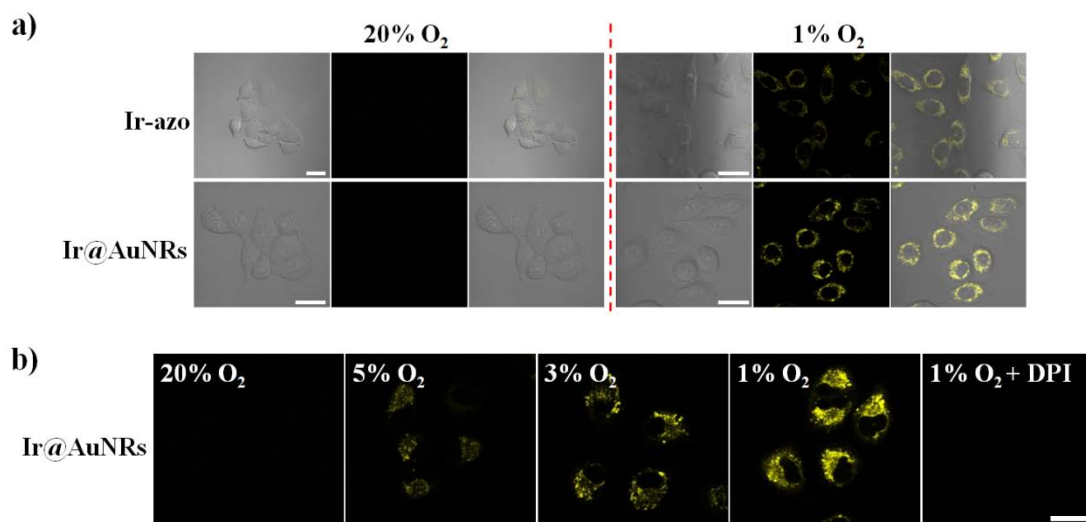


**Fig. S11** Confocal images of adherent A549 cells treated with **Ir-azo** (2.5  $\mu$ M, 0.5 h) and **Ir@AuNRs** (50  $\mu$ g/mL, 4 h) under normoxia (20% pO<sub>2</sub>) and hypoxia (1% pO<sub>2</sub>). Scale bar = 20  $\mu$ m. b) Confocal images of A549 cells to different O<sub>2</sub> concentration by **Ir@AuNRs** (50  $\mu$ g/mL, 4 h). Scale bar = 20  $\mu$ m.

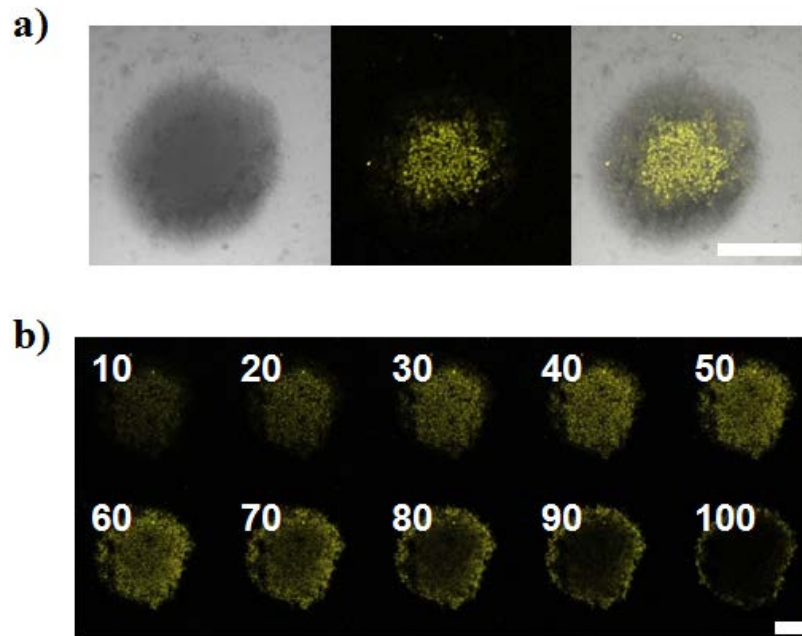


**Fig. S12** a) Confocal images of 3D multicellular spheroids incubated with **Ir@AuNRs** (50  $\mu\text{g/mL}$ ). Scale bar = 300  $\mu\text{m}$ . (b) Scanned Z-axis for 3D spheroids at 10  $\mu\text{m}$  intervals. Scale bar = 300  $\mu\text{m}$ .

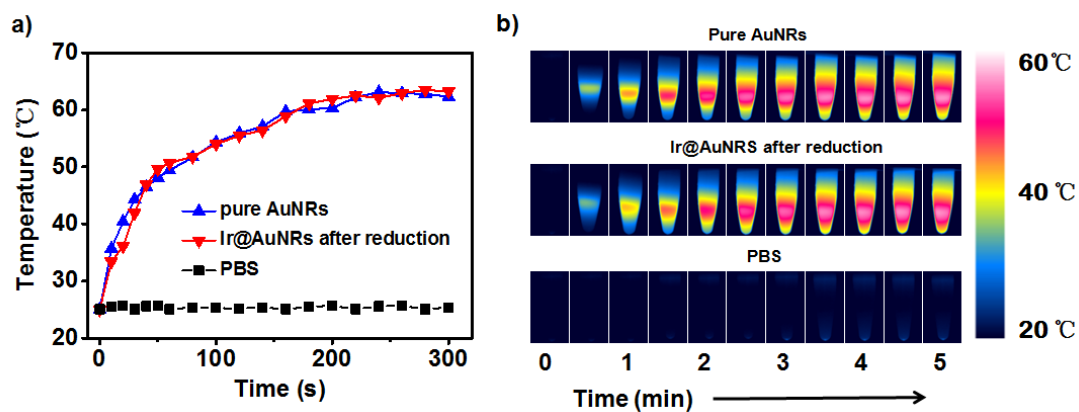


**Fig. S13** a) Temperature change and b) corresponding IR thermal images of **AuNRs**, **Ir@AuNRs** and **PBS** under NIR laser (808 nm, 0.8 W/cm<sup>2</sup>) irradiation.

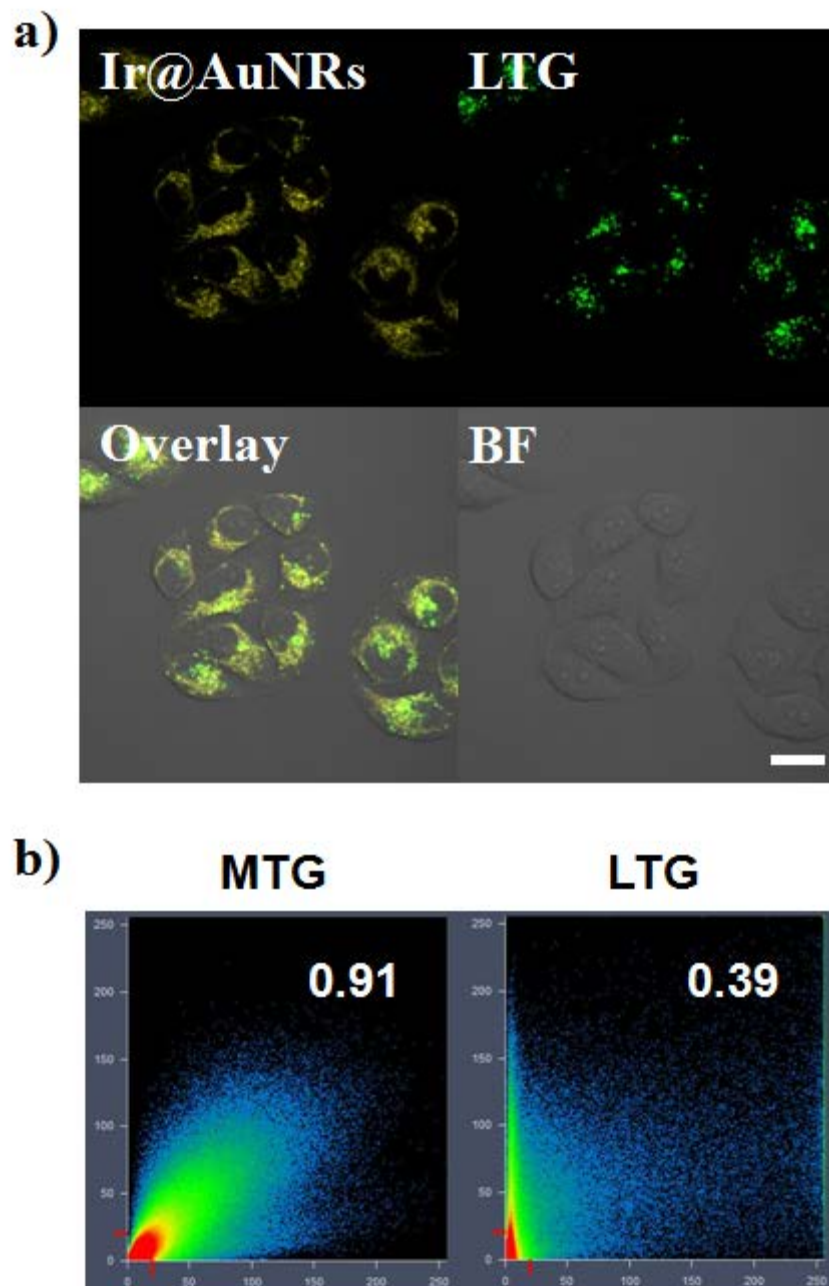


**Fig. S14** a) Confocal images of A549 cells co-labelled with Ir@AuNRs (50  $\mu\text{g}/\text{mL}$ ) and LTG (50 nM). Scale bar: 20  $\mu\text{m}$ . b) Pearson's coefficient of Ir@AuNRs co-labelled with MTG or LTG.

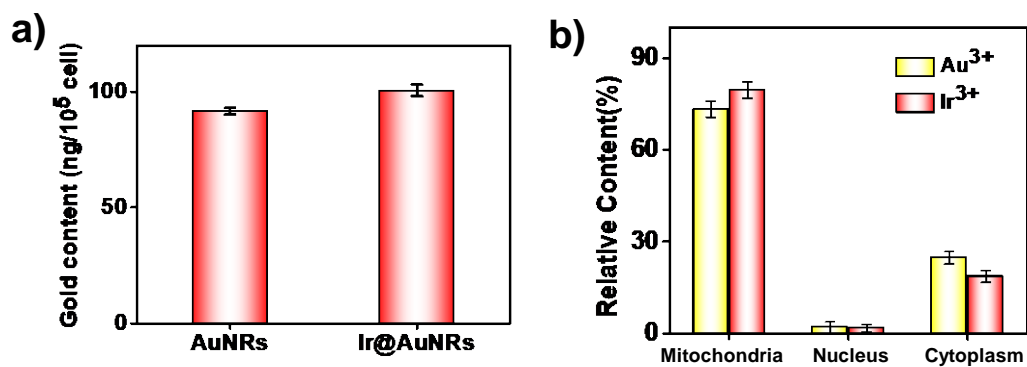


**Fig. S15** a) ICP-MS results of gold content internalized in to A549 cells for **AuNRs** (50  $\mu\text{g}/\text{mL}$ ) and **Ir@AuNRs** (50  $\mu\text{g}/\text{mL}$ ). b) The internalized gold and iridium content of the A549 cells were quantified by ICP-MS after 4 h treatment.

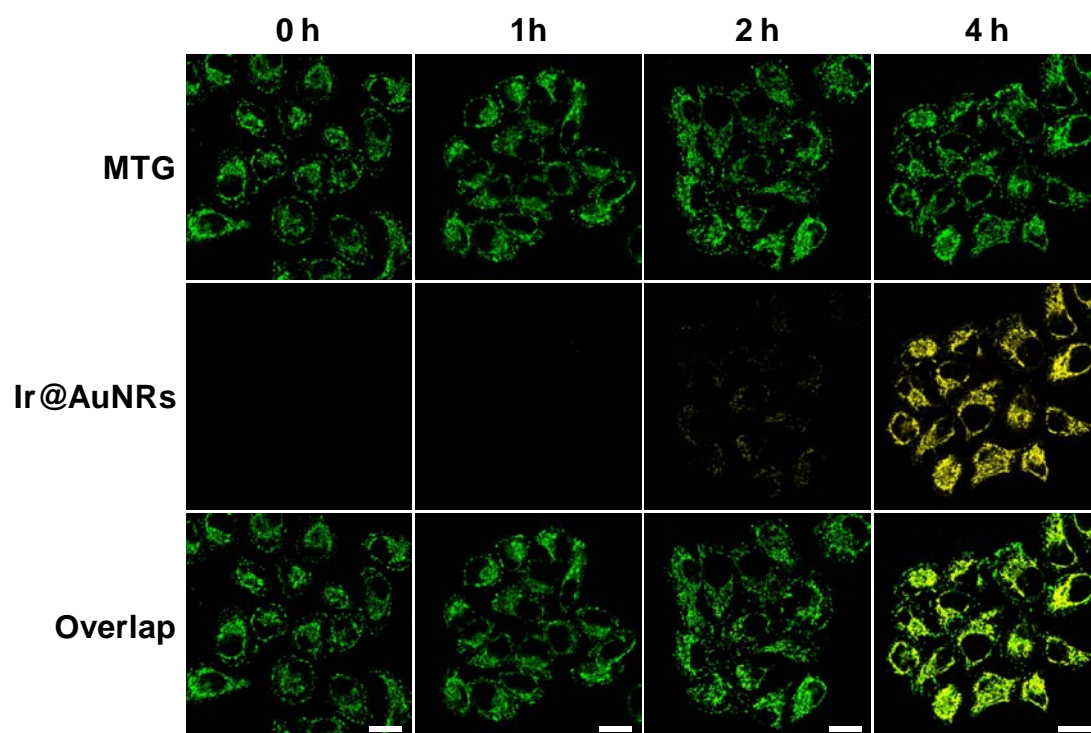


**Fig. S16** Confocal images of A549 cells co-labelled with **Ir@AuNRs** (50  $\mu\text{g}/\text{mL}$ ) and MTG (50 nM) were captured at different time points. Scale bar: 20  $\mu\text{m}$ .

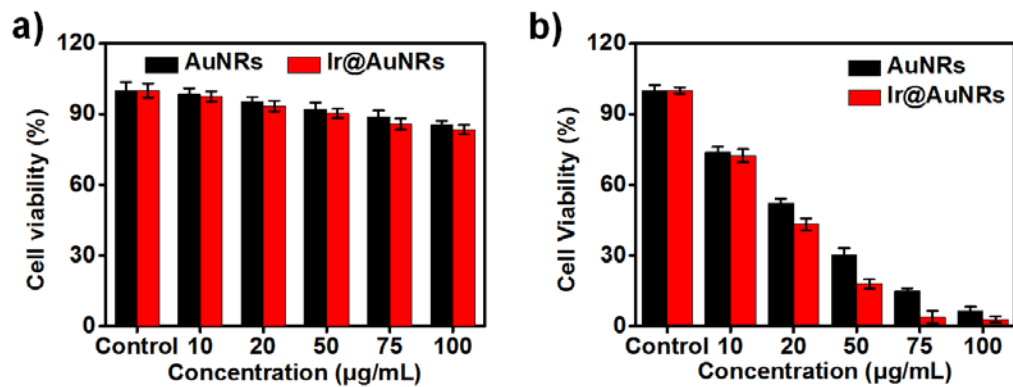


**Fig. S17** Cell viability of HeLa cells treated with different concentrations of **Ir@AuNRs** under hypoxia a) without or b) with NIR laser (808 nm, 0.8 W/cm<sup>2</sup>) irradiation.

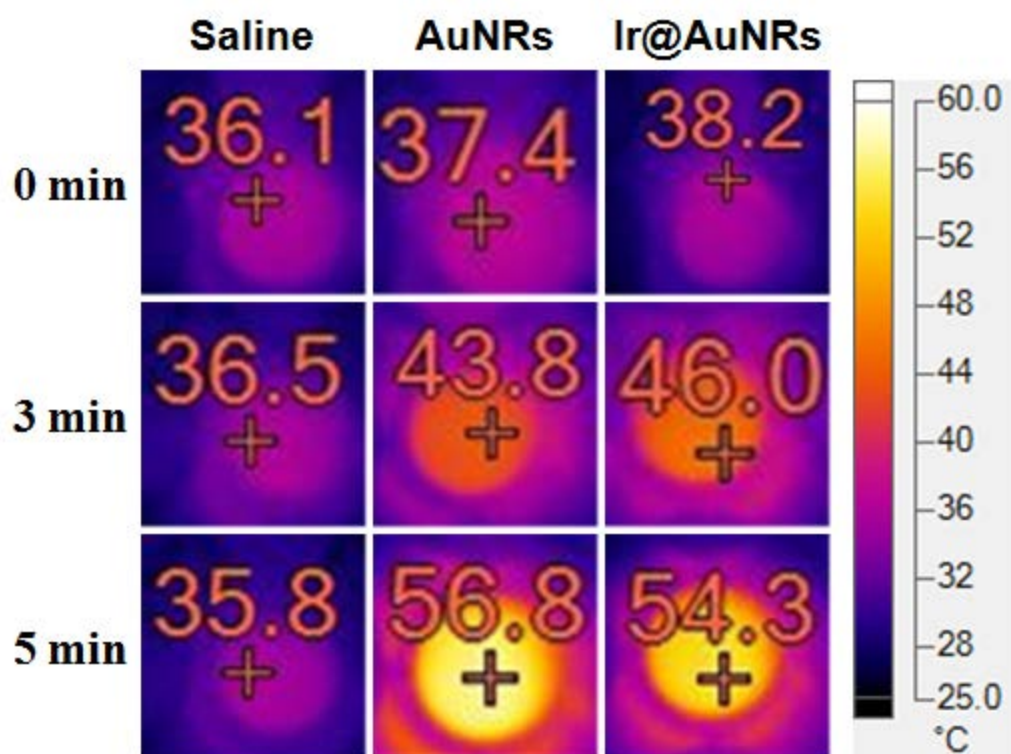


**Fig. S18** The photographs of real-time heating temperature of **AuNRs** and **Ir@AuNRs** *in vitro* (50  $\mu\text{g/mL}$ , 0.8  $\text{W/cm}^2$ ).

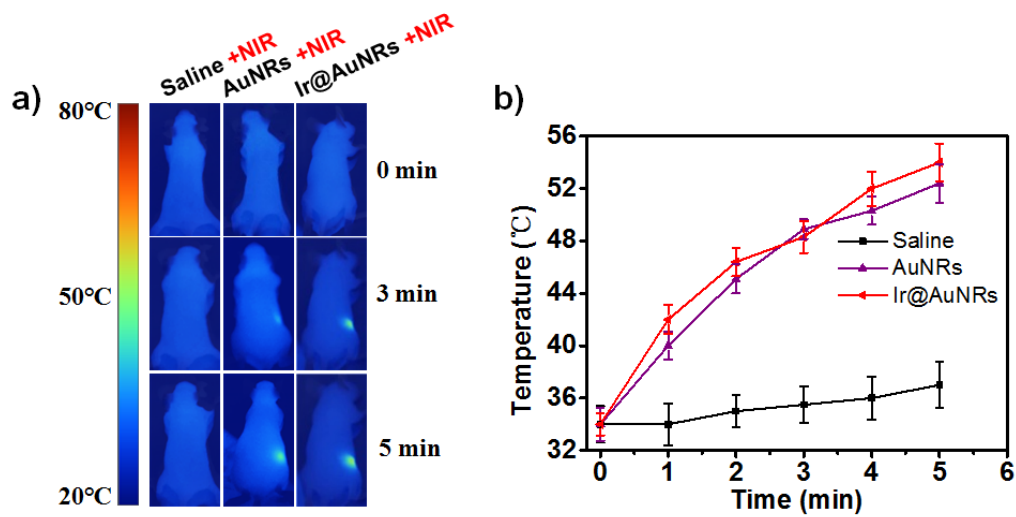


**Fig. S19** Photothermal effect of **AuNRs** and **Ir@AuNRs** *in vivo*. a) IR thermal images and b) Real-time temperature changes of **AuNRs** (1 mg/kg) and **Ir@AuNRs** (1 mg/kg) under the laser irradiation at the power density of 0.8 W/cm<sup>2</sup>.

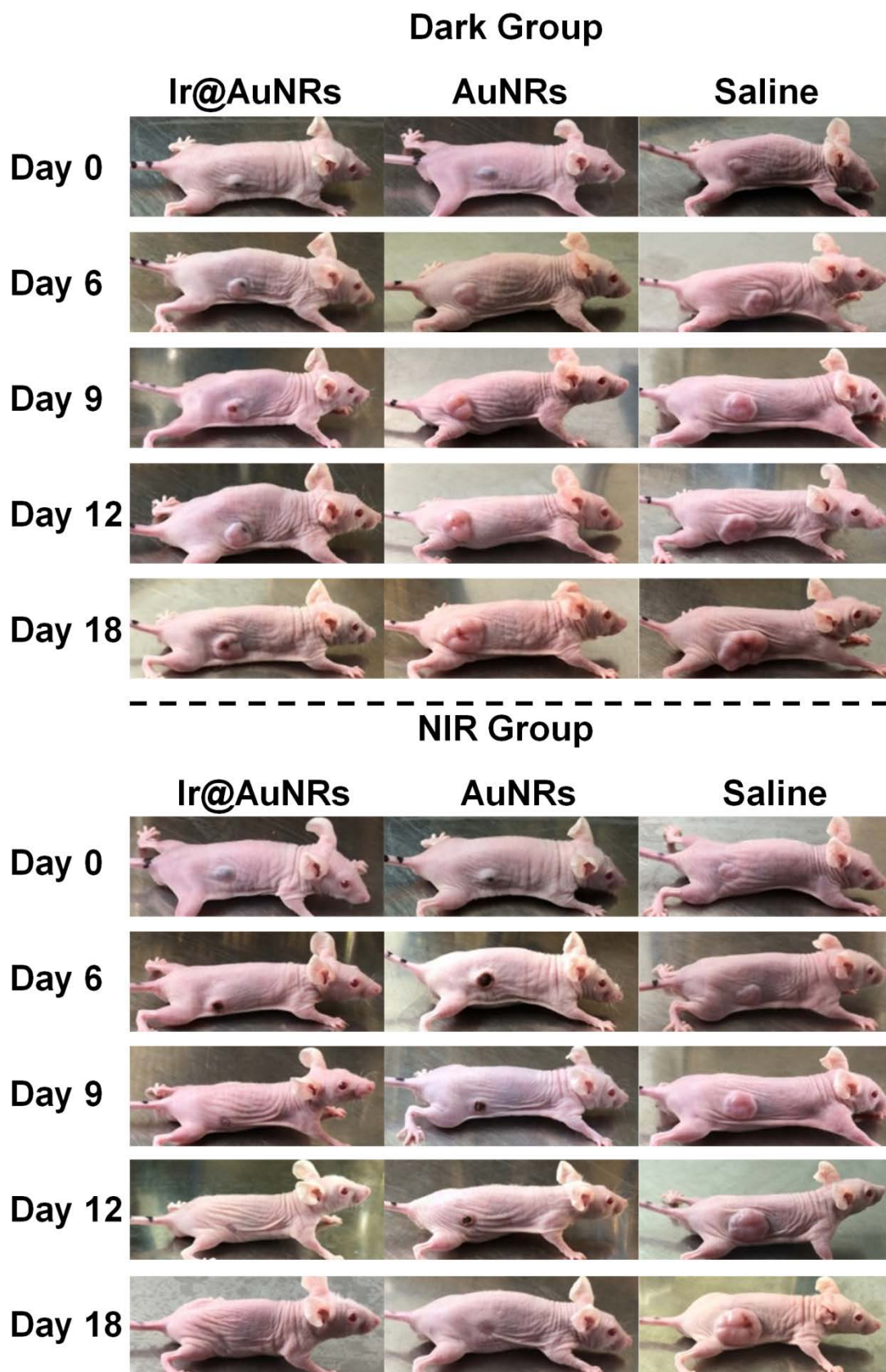


**Fig. S20** Representative photographs of A549 tumor-bearing mice before and after various treatments for days.

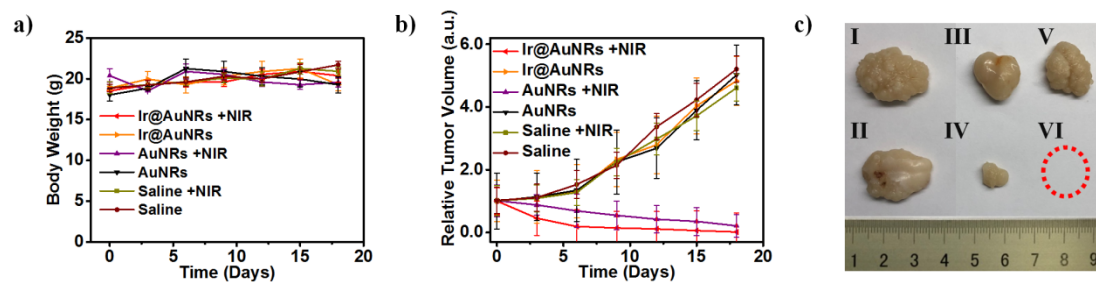


**Fig. S21** *In vivo* antitumor effect. a) Growth curve of tumor volume and b) Body weight of mice after intratumorally injection as indicated. c) Representative photographs of dissected tumors at 18 days post treatments. (I) Saline, (II) Saline + NIR, (III) AuNRs, (IV) AuNRs+ NIR, (V) Ir@AuNRs, (VI) Ir@AuNRs + NIR.

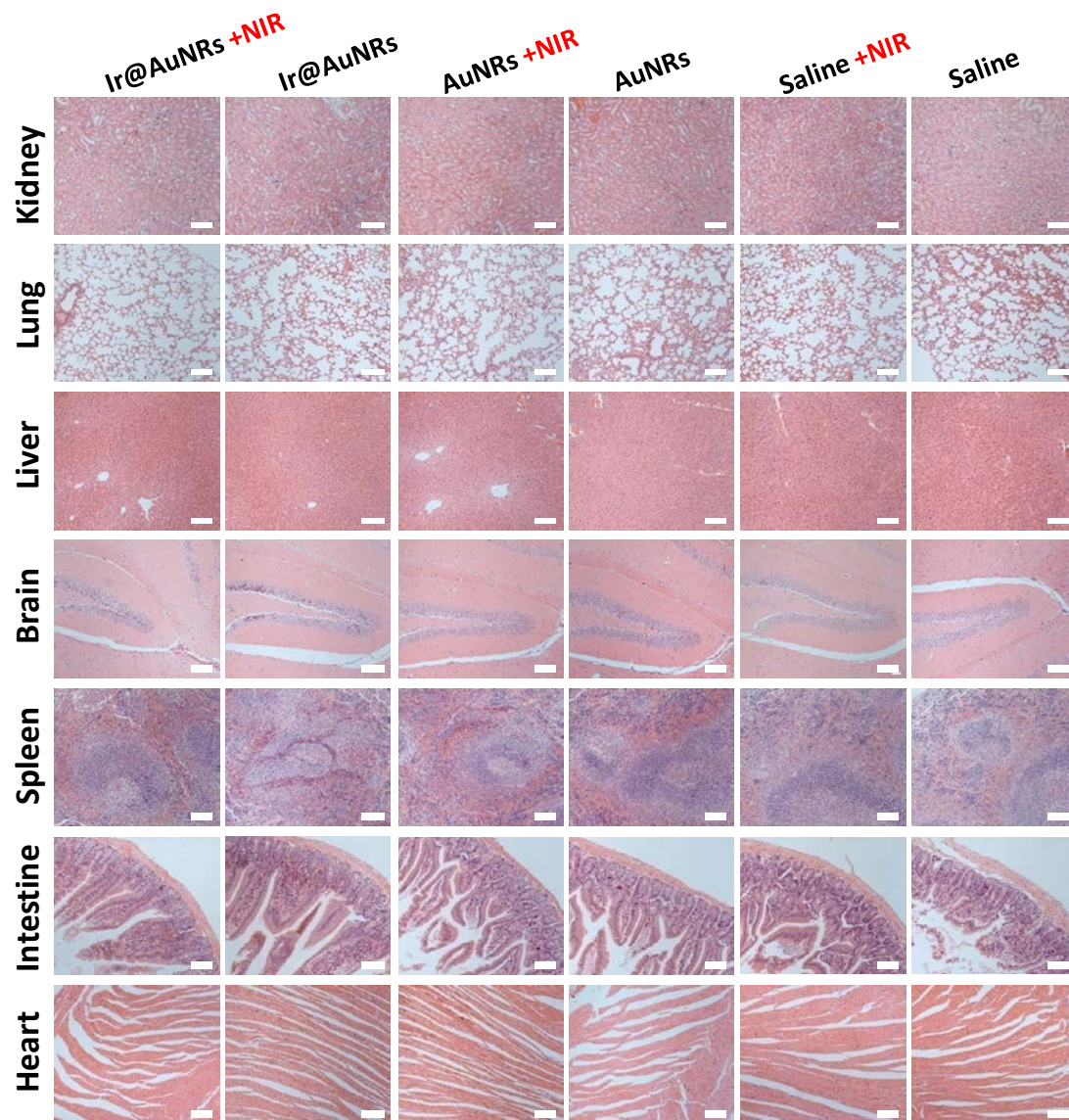


**Fig. S22** Histological examination of the major organs (kidney, lung, liver, brain, spleen, intestine and heart) after the various treatments. Sections for light microscopy were stained with hematoxylin-eosin (H&E) 18 days after the various treatments. (Scale bar: 50  $\mu\text{m}$  for all images).